Particle entry into the inner magnetosphere during duskward IMF By : Global three-dimensional electromagnetic full particle simulations

D. Cai, X.Y. Yan, K.-I. Nishikawa, Bertrand Lembège

Particle entry into the inner magnetosphere during duskward IMF B_y: Global three-dimensional electromagnetic full particle simulations

D. Cai,[1] X. Y. Yan,[1] K.-I. Nishikawa,[2] and B. Lembege[3]

Received 16 May 2005; revised 24 March 2006; accepted 3 May 2006; published 17 June 2006.

[1] The change of the interplanetary magnetic field (IMF) direction from northward to duskward has an important impact on the inner magnetosphere. This impact is analyzed with the help of a new parallel version of the global three-dimensional full particle simulation code. For northward IMF, bands of weak magnetic field (sash) form poleward of the cusp at high latitudes in each hemisphere. These sashes move to the equator (within opposite quadrants) as the IMF rotates duskward and merge into one another to form the characteristic "Crosstail-S" within the neutral sheet of the magnetotail. These macroscopic magnetic patterns (sashes and Crosstail-S) evidenced herein are in a good agreement with results of previous 3D MHD simulations and experimental observations. Moreover, the analysis of particle fluxes shows that "sashes" and "Crosstail-S" act as magnetic groove to facilitate the entry and injection of magnetosheath particles into the inner magnetosphere. Injected particles are accelerated after the IMF changes its direction from northward to duskward. **Citation:** Cai, D., X. Y. Yan, K.-I. Nishikawa, and B. Lembege (2006), Particle entry into the inner magnetosphere during duskward IMF B_y: Global three-dimensional electromagnetic full particle simulations, *Geophys. Res. Lett.*, *33*, L12101, doi:10.1029/2005GL023520.

1. Introduction

[2] Magnetospheric sashes in magnetopause and related phenomena have been observed and reported in some satellite observations [*Maynard et al.*, 2001], in global 3D MHD simulations [*White et al.*, 1998; *Siscoe et al.*, 2001] and in previous global three dimensional electromagnetic particle (3DEMP) simulations with dawnward IMF B_y [*Nishikawa*, 1998], that showed reconnection at the cusps and the flanks. This reconnection is expected to facilitate the magnetosheath particle entry into the plasma sheet directly, that is consistent with Geotail observations [*Fujimoto et al.*, 1997], but has not been verified yet in numerical simulations within a full self-consistent approach. The sash magnetic field structure at the near-Earth magnetotail with dawnward and duskward IMF B_y is also consistent with IMP 8 observations [*Kaymaz et al.*, 1994a, 1994b, 1995].

[3] In this letter, we perform simulation of the terrestrial magnetosphere using a new parallel version of our global three-dimensional electromagnetic particle code [*Cai et al.*, 2003] in order to investigate the self-consistent kinetic processes. We report new preliminary results from our simulations with duskward IMF B_y that address the following questions which have not yet been resolved: (i) can magnetic "sashes" be evidenced locally in the cusp region for a northward IMF; (ii) what is the temporal dynamics of sashes after the IMF rotates from northward to duskward and interacts with the magnetosphere?; (iii) how do these structures evolve spatially and in time between the dayside cusp region and the magnetotail region during this interaction?; and (iv) what are the three dimensional particle fluxes changes associated with these structures within the inner magnetosphere?

2. Simulation Model

[4] In our simulation, we use the same initial conditions to form the magnetosphere [*Buneman*, 1993], the same radiating boundary conditions [*Lindman*, 1975] and the charge-conserving formulas [*Villasenor and Buneman*, 1992] as in our previous works [*Nishikawa*, 1997, 1998; *Nishikawa and Ohtani*, 2002]. Now the grid size $\Delta \simeq 0.5RE$, and $\Delta t = 1$ is the time step ($\omega_{pe}\,\Delta t = 0.12$). Here $\Delta = \Delta x = \Delta y = \Delta z$.

[5] Initially, we use about 36×10^6 electron-ion pairs, which corresponds to a uniform particle density of $\tilde{n} = 8.0$ pairs per cell across the simulation domain ($215\Delta \times 145\Delta \times 145\Delta$). All the simulation parameters are improved with respect to those used in previous works ($\Delta \simeq 1RE$, $\omega_{pe}\,\Delta t = 0.2$, $\tilde{n} = 4$ pair per cell in [*Cai et al.*, 2003], or $\Delta \simeq 1RE$, $\omega_{pe}\,\Delta t = 0.84$, $\tilde{n} = 0.8$ pair per cell in [*Nishikawa*, 1998]). Here "$\sim$" denotes the normalized parameters defined as following ("e, and i" denotes electron and ion, respectively):

[6] Thermal velocity: $\tilde{v}_{the,i} = \frac{v_{the,i}}{\Delta/\Delta t}$ Debye length: $\tilde{\lambda}_{De,i} = \frac{\tilde{v}_{the,i}}{\tilde{\omega}_{pe,i}}$, Larmor gyroradius: $\tilde{\rho}_{ce,i} = \frac{\tilde{v}_{the,i}}{\tilde{\omega}_{ce,i}}$, Inertia length: $\tilde{\lambda}_{ce,i} = \frac{\tilde{C}}{\tilde{\omega}_{pe,i}}$, Gyrofrequency: $\tilde{\omega}_{ce,i} = \frac{\omega_{ce,i}}{(\Delta t)^{-1}} = \frac{\tilde{B}\Delta m_e}{\Delta t\, m_{e,i}}$, Plasma frequency: $\tilde{\omega}_{pe,i} = \frac{\omega_{pe,i}}{(\Delta t)^{-1}} = \sqrt{\frac{\tilde{q}_{e,i}^2 \tilde{n}_{e,i}}{\varepsilon_0 \tilde{m}_{e,i}}}\Delta t$, Gyroperiod: $\tilde{\tau}_{ce,i} = \frac{2\pi}{\tilde{\omega}_{ce,i}}$, β ratio: $\tilde{\beta}_{ce,i} = \frac{\tilde{T}_{e,i}\tilde{\omega}_{pe,i}^2}{\tilde{B}^2}$. Values of normalized ambient plasma parameters used in our simulation are following: $\tilde{v}_{the,i}$ = (0.09, 0.045), $\tilde{\lambda}_{De,i}$ = (0.75, 1.5), $\tilde{\omega}_{pe,i}$ = (0.125, 0.031), $\tilde{\omega}_{ce,i}$ = (0.20, 0.013), $\tilde{\rho}_{ce,i}$ = (0.45, 3.5), $\frac{\tilde{C}}{\tilde{\omega}_{pe,i}}$ = (4.2, 16.1), $\tilde{\tau}_{ce,i}$ = (31.4, 502), $\tilde{\beta}_{e,i}$ = (0.2, 0.8), $\tilde{T}_{e,i}$= (0.008, 0.032). The center of the current loop that generates the dipolar terrestrial magnetic field is located at (80Δ, 72.5Δ, 73Δ). Within the time range $0 < \tilde{t} < 1000\Delta\tilde{t}$, a drift velocity

[1]Graduate School of Systems and Information Engineering, University of Tsukuba, Tsukuba, Japan.
[2]National Space Science and Technology Center, Huntsville, Alabama, USA.
[3]Centre d'Etude des Environnements Terrestre et Planétaires/ Universitéde Versailles Saint-Quentin-en-Yvelines/L'Institut Pierre-Simon Laplace, Velizy, France.

0094-8276/06/2005GL023520

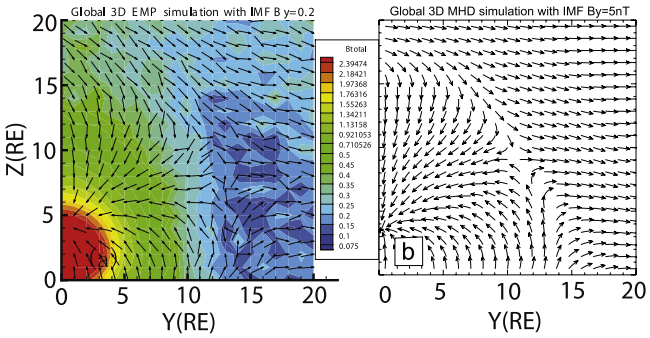

Figure 1. *Y-Z* sectional slices of magnetic field vector with duskward IMF *B*y (>0) near magnetotail at $x = -5R$E. Results are issued from (a) our global 3D EMP simulation with IMF *B*y = 0.2 at $\tilde{t} = 4000\Delta\tilde{t}$ (isocolors correspond to total B field values), and (b) global 3D MHD simulation with IMF *B*y = 5*nT* [*White et al.*, 1998].

$\tilde{v}_{sol} = -0.5\tilde{c}$ representing the solar wind, is applied along the x-direction without an IMF. Here $\tilde{c} = 0.5$ is the speed of light. The injected solar wind density has also $\tilde{n} = 8.0$ electron-ion pairs per cell, the mass ratio is $m_i/m_e = 16$, and the electron and ion thermal velocities are $\tilde{v}_{the} = (\tilde{T}_e/m_e)^{1/2} = 0.18\tilde{c}$, and $\tilde{v}_{the} = (\tilde{T}_i/m_i)^{1/2} = 0.09\tilde{c}$, respectively. The electron plasma frequency $\tilde{\omega}_{pe} = 0.12$.

3. Simulation Results

[7] A quasi-steady state is established with an unmagnetized solar wind, at time $\tilde{t} = 1000\Delta\tilde{t}$. A northward IMF with $\tilde{B}^{IMF}{}_z = 0.2$ is switched on gradually and smoothly at $x = 0$ during the time interval $1001\Delta\tilde{t} < \tilde{t} < 1400\Delta\tilde{t}$, while the solar wind is continuously applied. At time $\tilde{t} = 2260\Delta\tilde{t}$, the northward IMF $B^{\mathrm{IMF}}{}_z$ carried by the solar wind prevails within the whole simulation domain. Then, at $x = 0$, we gradually rotate the IMF from northward to duskward $B^{\mathrm{IMF}}{}_y$ between $\tilde{t} = 2400\Delta t$ and $\tilde{t} = 2800\Delta t$ keeping its amplitude constant $\tilde{B}^{\mathrm{IMF}} = 0.2$. The *Alfvén* velocity with this $\tilde{B}^{\mathrm{IMF}}{}_y$ is $\tilde{v}_A/\tilde{c} = 0.39$. This procedure strongly differs from that used in our previous works, where the $B^{\mathrm{IMF}}{}_y$ was suddenly applied (no rotation), and allows us to analyze in detail the latter impact of the IMF rotation into the inner magnetosphere by a more realistic way.

[8] An enlarged projection of the terrestrial magnetosphere is plotted in Figure 1a at time $\tilde{t} = 4000\Delta\tilde{t}$ within the cross sectional plane Y-Z perpendicular to the solar wind flow and located at $x = -5R$E (night side). The duskward $B^{\mathrm{IMF}}{}_y$ prevails in the whole inner magnetosphere by that time. A "separatrix" in the B vectors direction is clearly evidenced around the location (y, z) = (12, 9) *R*E ("X" topology in the Y-Z plane), i.e., at the lower edge of the minimum-B field region ("dark blue" area in Figure 1a), which corresponds to the slicing of a 3-D minimum magnetic field band (so-called "sash"). The configuration of B vectors found herein is in a good agreement with previous results of 3D MHD simulation [*White et al.*, 1998, Figure 1b], which allows us to validate our present results. As the B^{IMF} is northward, two sashes are located in each hemisphere, and are aligned along a north-south axis. The two sashes are located poleward of the cusps at high altitude and persist at the high latitude magnetopause tailward of the cusp. These do not connect each other in the tail as this will occur for a fully dawn-dusk oriented $B^{\mathrm{IMF}}{}_y$. This north-south axis rotates within the Y-Z plane and stabilizes around the 45° direction as the newly oriented duskward $B^{\mathrm{IMF}}{}_y$ interacts progressively with the inner magnetosphere. The 45° direction results from the superposition of the $B^{\mathrm{IMF}}{}_y$ with the northward $B^{\mathrm{Terr}}{}_z$ terrestrial magnetic field, in a good agreement with previous MHD results of *Siscoe et al.* [2001].

[9] Figure 2 shows the ion and electron fluxes for $\tilde{t} = 4000\Delta t$ at $x = 5R$E (near the dayside magnetopause) and at $x = -5R$E (night side). Figures 2a and 2b show that a strong ion flux extends along the magnetopause at $x = 5R$E from (y, z) = (0, 10) *R*E to (7, 8) *R*E, while a strong electron flux extends from the (y, z) = (12, 0)*R*E to (7, 8)*R*E. The common location (7, 8)*R*E corresponds to the shifted region of the cusp located on the flank of the magnetopause on the basis of the magnetic field separatrix (circle in Figures 2a and 2b). It corresponds also to the beginning of the 3-D "sash" structure extending further within the magnetosphere. The situation differs in the nightside region (Figures 2c and 2d for $x = -5R$E), where both electron and ion fluxes are large in a region centered around (y, z) = (12, 13)*R*E, i.e., very near the "sash" location. Comparing intermediary plots (not shown here) between $x = 5R$E and $x = -5R$E at $t = 4000\Delta t$ confirms that these fluxes are still quite large near the "sash" region, i.e., the "sash" pattern acts as a magnetic "groove" along which particles are traveling from the cusp region (magnetopause flank) into the inner magnetosphere. Comparing the same plot at previous times (not shown here) confirms that this injection at this x location takes place immediately after the duskward

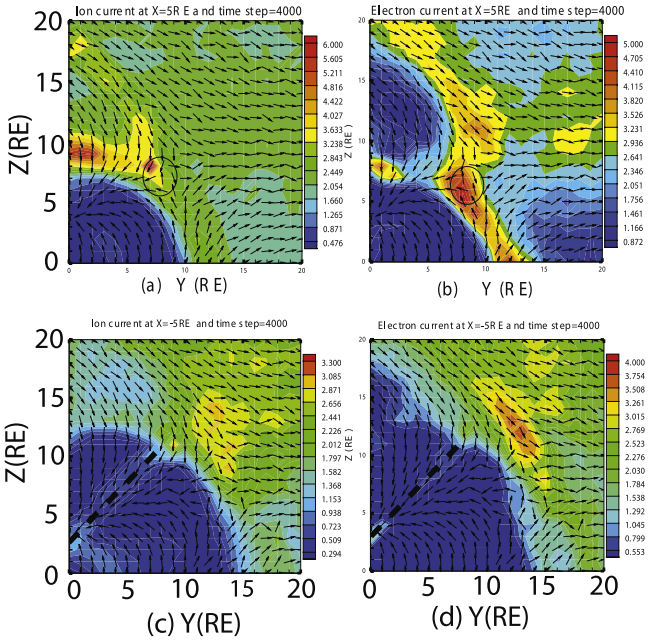

Figure 2. Sectional slices of the total electron and ion fluxes with magnetic field vectors measured at time $\tilde{t} = 4000\Delta\tilde{t}$ within the Y-Z plane located on the dayside at $x = 5R$E for (a) ions and (b) electrons, respectively, and (c and d) similar plots shown on the night side (near the magnetotail) at $x = -5R$E.

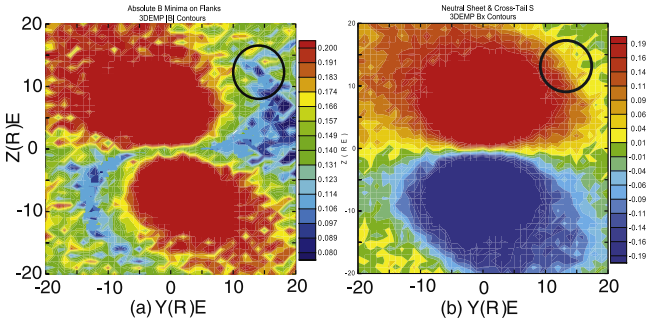

Figure 3. Y-Z sectional slices of the "crosstail-S" measured at $x = -10R$E at $\tilde{t} = 4000\Delta\tilde{t}$ are visualized in (a) B-magnitude contour (total B field); and in (b) B_x contour (Red = +Bx and blue = −Bx).

IMF has passed over this location $x = -5R$E. In addition, smaller but finite current flux (light 'blue color') is also evidenced within a particular band identified by the dashed line extending from the "sash" location (y, z) = (9,11)*R*E to (0, 3)*R*E. This band corresponds to another magnetic "groove" (herein well directed and finite magnetic field band evidenced in Figure 1a), along which some particles travel earthward from the cusp.

[10] In order to analyze the evolution of the "sash" pattern within the whole inner magnetosphere and to determine the corresponding behavior of electrons and ions, we have plotted similar slices at different locations within the more distant magnetotail at the same late time ($\tilde{t} = 4000\Delta\tilde{t}$). Intermediate slices made at different x-locations (not shown herein) clearly show that the sash pattern forms on the dayside magnetopause flanks and extends to the nearby magnetotail. This sash pattern is observed in the northern and southern hemispheres in opposite quadrants, i.e., on the dusk and the dawnside. "Sashes" gradually join onto neutral sheet locations, and merge into each other to form a geometrical feature called the "crosstail-S". This merging results from the fact that "sashes" approach the neutral sheet region in the tail during their rotation (tilt of their 45° axis). All "regions" of weak magnetic field (neutral sheet and "sash") merge as more easily as the amplitude of the magnetic field globally decreases when moving tailward and approaching the neutral sheet. Results are illustrated in Figure 3, which shows the cross sectional slices of (a) B-magnitude and (b) B_x contours at $x = -10R$E. A similar pattern has been already evidenced in our previous work (with much lower resolution) with dawnward IMF [*Nishikawa*, 1998], in previous global 3D MHD simulations [*White et al.*, 1998], and in IMP 8 observation [*Kaymaz et al.*, 1994a]. However, the higher spatial resolution used herein allows us to measure more precisely the location and the extent of the "crosstail-S" pattern which can be well evidenced in the tail region within the range $x = -10$ *R*E and $x = -16$ *R*E. This pattern becomes thinner, whose thickness $\Delta z \approx 1-2$ *R*E, within the neutral sheet around $x = -13$ *R*E, but progressively diffuses for larger distances from the Earth. This thickness is smaller than that by *Nishikawa* [1998] (thickness ≈6*R*E around $x = -15$ *R*E).

[11] Figure 4 shows the corresponding parallel fluxes components of (a) electrons and (b) ions, respectively with the magnetic field vectors at $\tilde{t} = 2400\Delta\tilde{t}$ (northward IMF) and $\tilde{t} = 4000\Delta\tilde{t}$ (duskward IMF) for $x = -10R$E. Both parallel ion and electron fluxes are very large around location (y, z) = (14, 13) *R*E for $\tilde{t} = 4000\Delta\tilde{t}$, which corresponds to the magnetospheric sash location (extremity of the "crosstail-S" in the circle in Figure 3a, whose detailed structures are reported in Figure 4). This agreement and the sign of the parallel flux components confirm that ions and electrons are injected via the magnetospheric "sashes" into the plasma sheet of the nearby magnetotail (B_x is still positive at the circle location in Figure 3b). Moreover, the amplitude of each parallel component at this location is much larger for $\tilde{t} = 4000\Delta\tilde{t}$ than for $\tilde{t} = 2400\Delta\tilde{t}$, which indicates that particles are injected and accelerated through the magnetic sash. In summary, present results reveal that the magnetospheric "sash" patterns provide a "road" for magnetosheath particles to enter into the inner magnetosphere (injection and acceleration), the plasma sheet and the current sheet, after IMF B_{IMF} rotates to the duskward direction.

4. Discussions

[12] Present new 3D EMP simulations show that a weak magnetic field band or "sash" forms poleward of the cusp at high latitude (in each hemisphere) for a northward IMF B_{IMF}. In this IMF configuration, these sashes are far each other and from the equatorial plane; these cannot merge within the near-Earth neutral sheet. After the IMF B_{IMF} rotates from northward to duskward direction, these "sashes" rotate out of the poleward direction within the plane perpendicular to the solar wind and stabilize around a tilted 45° axis, after $B^{IMF}{}_y$ has interacted with the magnetosphere. On the dayside ($x = 5R$E), electron and ion fluxes are strong along the magnetopause flanks but in different regions apart from the cusp region. When penetrating further in the night side and approaching the

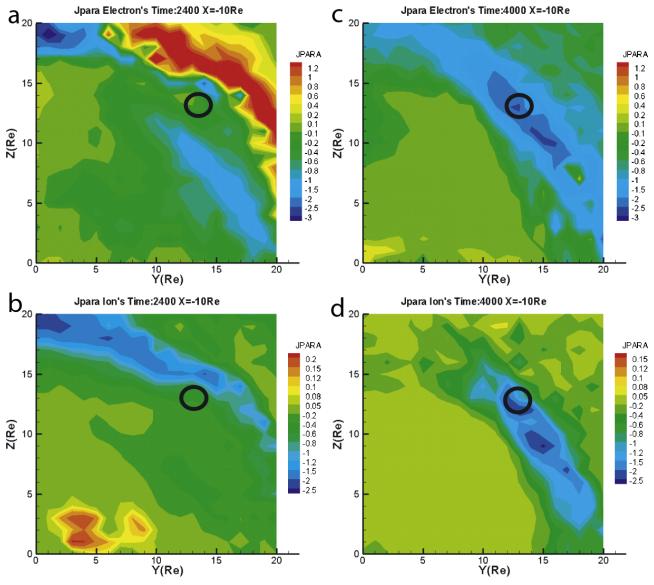

Figure 4. Parallel (a) electron and (b) ion flux components (isocolors) in our global 3DEMP simulation at $\tilde{t} = 2400\Delta\tilde{t}$ at $x = -10R$E. Parallel (c) electron and (d) ion flux components (isocolors) at $\tilde{t} = 4000\Delta\tilde{t}$.

near magnetotail, two important processes take place. First, the ''sashes'' approach each other along the tilted 45° axis and merge progressively to join the neutral sheet in the tail. Then they form a characteristic ''crosstail-S''. These results are similar to those of *Siscoe et al.* [2001], obtained with MHD simulations (IMF rotation of 90°). Herein, the spatial extent of the ''crosstail-S'' pattern is limited within the range $x = -10R$E to -16 RE which corresponds to the nearby magnetotail. As a result, these ''sash'' patterns establish a link from the magnetopause flanks (top cusp) in the dayside, to the inner magnetosphere (neutral sheet in the tail) in the night side. Second, both electrons and ions use this magnetospheric ''sash'' as a ''groove'' to penetrate the inner magnetosphere from the top cusp (nearby magnetopause) to the inner plasma sheet. Both particle species are injected and accelerated along this ''road''. We believe that these ''sash'' patterns caused by the duskward IMF B_y component are essential for direct plasma entry into the inner magnetosphere and neutral sheet [*Fujimoto et al.*, 1997; *Nishikawa*, 1998; *White et al.*, 1998; *Kaymaz et al.*, 1994a, 1995]. Multi-points measurements of CLUSTER II mission can represent an excellent opportunity to identify the characteristic sash topology and the dynamics of the associated flux currents.

[13] **Acknowledgments.** The simulation of our parallel three-dimensional electromagnetic particle code was performed in VPP5000 supercomputers in both the Information Center of University of Tsukuba and in Computer the Center of Nagoya University. K.I.N is partially supported by NSF ATM-0100997, and INT-9981508. K.I.N thanks M. Chandlar for fruitful discussion. The authors wish to thank one of the referees for helpful comments. This work has been finalized during the stay at Tsukuba University of one of the author (BL) who thanks JSPS for his financial support.

References

Buneman, O. (1993), TRISTAN, in *Computer Space Plasma Physics: Simulation Techniques and Software*, edited by H. Matsumoto and Y. Omura, pp. 67–84, Terra Sci., Tokyo.

Buneman, O., K.-I. Nishikawa, and T. Neubert (1995), Solar wind-magnetosphere interaction as simulated by a 3D EM particle code, in *Space Plasmas: Coupling Between Small and Medium Scale Processes*, *Geophys. Monogr. Ser.*, vol. 86, edited by M. Ashour-Abdalla, T. Chang, and P. Dusenburg, pp. 347–352, AGU, Washington, D. C.

Cai, D. S., Y. Li, K. H. Nishikawa, C. Xiao, X. Yan, and Z. Pu (2003), Parallel 3D electromagnetic particle code using high performance Fortran: Parallel TRISTAN, in *Space Plasma Simulation*, pp. 25–53, Springer, New York.

Fujimoto, M., T. Mukai, A. Matsuoka, A. Nishida, T. Terasawa, K. Seki, H. Hayakawa, T. Yamamoto, S. Kokubun, and R. P. Lepping (1997), Dayside reconnection field lines in the southdusk near-tail flank during an IMF $By > 0$ dominated period, *Geophys. Res. Lett.*, *24*, 931–934.

Kaymaz, Z., G. L. Siscoe, N. A. Tsyganenko, and P. P. Lepping (1994a), Magnetotail views at 33RE: IMP 8 magnetometer observations, *J. Geophys. Res.*, *99*(A5), 8705–8730.

Kaymaz, Z., G. L. Siscoe, J. G. Luhmann, R. P. Lepping, and C. T. Russell (1994b), Interplanetary magnetic field control of magnetotail magnetic field geometry: IMP 8 observations, *J. Geophys. Res.*, *99*(A6), 11,113–11,126.

Kaymaz, Z., G. Siscoe, J. G. Luhmann, J. A. Fedder, and J. G. Lyon (1995), Interplanetary magnetic field control of magnetotail field: IMP 8 data and MHD model compared, *J. Geophys. Res.*, *100*(A9), 17,163–17,172.

Lindman, E. L. (1975), Free-space boundary conditions for the time dependent wave equation, *J. Comput. Phys.*, *18*, 66–78.

Maynard, N. C., et al. (2001), Observation of the magnetospheric ''sash'' and its implications relative to solar-wind/magnetospheric coupling: A multisatellite event analysis, *J. Geophys. Res.*, *106*(A4), 6097–6122.

Nishikawa, K.-I. (1997), Particle entry into the magnetosphere with a southward IMF as simulated by a 3D EM particle code, *J. Geophys. Res.*, *102*, 17,631–17,642.

Nishikawa, K.-I. (1998), Particle entry through reconnection grooves in the magnetopause with a dawnward IMF as simulated by a 3D EM particle code, *Geophys. Res. Lett.*, *25*, 1609–1612.

Nishikawa, K.-I., and S. Ohtani (2002), Particle simulation study of substorm triggering with a southward IMF, *Adv. Space Res.*, *30*(12), 2675–2681.

Siscoe, G. L., G. M. Erickson, B. U. O. Sonnerup, N. C. Maynard, K. D. Siebert, D. R. Weimer, and W. W. White (2001), Magnetospheric sash dependance on IMF direction, *Geophys. Res. Lett.*, *28*(10), 1921–1924.

Villasenor, J., and O. Buneman (1992), Rigorous charge conservation for local electromagnetic field solvers, *Comput. Phys. Commun.*, *69*, 306–316.

White, W. W., G. L. Siscoe, G. M. Erickson, Z. Kaymaz, N. C. Maynard, K. D. Siebert, B. U. O. Sonnerup, and D. R. Weimer (1998), The magnetospheric sash and the cross-tail S, *Geophys. Res. Let.*, *25*, 1605–1608.

D. Cai and X. Y. Yan, Graduate School of Systems and Information Engineering, University of Tsukuba, Tsukuba, 305-8573 Ibaraki, Japan.

B. Lembege, Centre d'Etude des Environnements Terrestre et Planétaires/ Université de Versailles Saint-Quentin-en-Yvelines/L'Institut Pierre-Simon Laplace, 10–12 Avenue de l'Europe, FR-78140 Velizy, France.

K.-I. Nishikawa, National Space Science and Technology Center, 320 Sparkman Drive, Huntsville, AL 35805, USA.